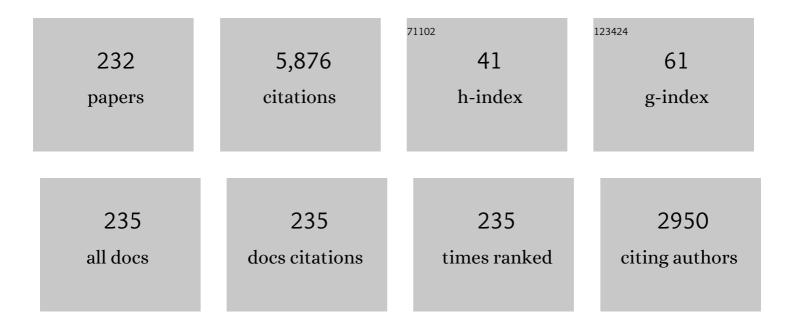
Graham J Nathan

List of Publications by Year in descending order

Source: https://exaly.com/author-pdf/5708847/publications.pdf Version: 2024-02-01



#	Article	IF	CITATIONS
1	Operational characteristics of a parallel jet MILD combustion burner system. Combustion and Flame, 2009, 156, 429-438.	5.2	179
2	Scaling of NOx emissions from a laboratory-scale mild combustion furnace. Combustion and Flame, 2008, 154, 281-295.	5.2	140
3	Centreline mixing characteristics of jets from nine differently shaped nozzles. Experiments in Fluids, 2000, 28, 93-94.	2.4	138
4	A Review of Terminology Used to Describe Soot Formation and Evolution under Combustion and Pyrolytic Conditions. ACS Nano, 2020, 14, 12470-12490.	14.6	122
5	Soot volume fraction in a piloted turbulent jet non-premixed flame of natural gas. Combustion and Flame, 2009, 156, 1339-1347.	5.2	117
6	Impacts of a jet's exit flow pattern on mixing and combustion performance. Progress in Energy and Combustion Science, 2006, 32, 496-538.	31.2	116
7	Solar thermal hybrids for combustion power plant: A growing opportunity. Progress in Energy and Combustion Science, 2018, 64, 4-28.	31.2	110
8	The influence of Reynolds number on a plane jet. Physics of Fluids, 2008, 20, .	4.0	108
9	PIV measurements of a turbulent jet issuing from round sharp-edged plate. Experiments in Fluids, 2007, 42, 625-637.	2.4	106
10	The release of water-bound and organic sodium from Loy Yang coal during the combustion of single particles in a flat flame. Combustion and Flame, 2011, 158, 1181-1192.	5.2	106
11	Influence of Stokes number on the velocity and concentration distributions in particle-laden jets. Journal of Fluid Mechanics, 2014, 757, 432-457.	3.4	94
12	Mechanism and kinetics of sodium release from brown coal char particles during combustion. Combustion and Flame, 2011, 158, 2512-2523.	5.2	86
13	The influence of nozzle aspect ratio on plane jets. Experimental Thermal and Fluid Science, 2007, 31, 825-838.	2.7	80
14	Effects of hydrogen and nitrogen on soot volume fraction, primary particle diameter and temperature in laminar ethylene/air diffusion flames. Combustion and Flame, 2017, 175, 270-282.	5.2	77
15	The effect of Stokes number on particle velocity and concentration distributions in a well-characterised, turbulent, co-flowingÂtwo-phase jet. Journal of Fluid Mechanics, 2016, 809, 72-110.	3.4	75
16	Recent advances in the measurement of strongly radiating, turbulent reacting flows. Progress in Energy and Combustion Science, 2012, 38, 41-61.	31.2	72
17	The influence of nozzle-exit geometric profile on statistical properties of a turbulent plane jet. Experimental Thermal and Fluid Science, 2007, 32, 545-559.	2.7	70
18	Sodium and Potassium Released from Burning Particles of Brown Coal and Pine Wood in a Laminar Premixed Methane Flame Using Quantitative Laser-Induced Breakdown Spectroscopy. Applied Spectroscopy, 2011, 65, 684-691.	2.2	68

#	Article	IF	CITATIONS
19	Quantitative measurement of atomic sodium in the plume of a single burning coal particle. Combustion and Flame, 2008, 155, 529-537.	5.2	64
20	A hybrid solar and chemical looping combustion system for solar thermal energy storage. Applied Energy, 2013, 103, 671-678.	10.1	63
21	Potential use of liquid metal oxides for chemical looping gasification: A thermodynamic assessment. Applied Energy, 2017, 195, 702-712.	10.1	63
22	A pressurized high-flux solar reactor for the efficient thermochemical gasification of carbonaceous feedstock. Fuel, 2017, 193, 432-443.	6.4	61
23	The effect of global mixing on soot volume fraction: measurements in simple jet, precessing jet, and bluff body flames. Proceedings of the Combustion Institute, 2005, 30, 1493-1500.	3.9	57
24	Development of temperature imaging using two-line atomic fluorescence. Applied Optics, 2009, 48, 1237.	2.1	57
25	A Novel Solar Expanding-Vortex Particle Reactor: Influence of Vortex Structure on Particle Residence Times and Trajectories. Solar Energy, 2015, 122, 58-75.	6.1	56
26	The influence of probe resolution on the measurement of a passive scalar and its derivatives. Experiments in Fluids, 2003, 34, 687-696.	2.4	55
27	Comparison of turbulent jets issuing from rectangular nozzles with and without sidewalls. Experimental Thermal and Fluid Science, 2007, 32, 596-606.	2.7	55
28	Experimental and computational study of soot evolution in a turbulent nonpremixed bluff body ethylene flame. Combustion and Flame, 2013, 160, 1298-1309.	5.2	55
29	Economic evaluation of a novel fuel-saver hybrid combining a solar receiver with a combustor for a solar power tower. Applied Energy, 2014, 113, 1235-1243.	10.1	55
30	Temporal release of potassium from pinewood particles during combustion. Combustion and Flame, 2015, 162, 496-505.	5.2	55
31	Simultaneous measurements of gas temperature, soot volume fraction and primary particle diameter in a sooting lifted turbulent ethylene/air non-premixed flame. Combustion and Flame, 2017, 179, 33-50.	5.2	51
32	Simultaneous planar measurements of temperature and soot volume fraction in a turbulent non-premixed jet flame. Proceedings of the Combustion Institute, 2015, 35, 1931-1938.	3.9	50
33	Simultaneous measurements of the release of atomic sodium, particle diameter and particle temperature for a single burning coal particle. Proceedings of the Combustion Institute, 2009, 32, 2099-2106.	3.9	49
34	Polygeneration of Liquid Fuels and Electricity by the Atmospheric Pressure Hybrid Solar Gasification of Coal. Energy & Fuels, 2013, 27, 3538-3555.	5.1	49
35	Time-resolved spectra of solar simulators employing metal halide and xenon arc lamps. Solar Energy, 2015, 115, 613-620.	6.1	47
36	Single-shot, Time-Resolved planar Laser-Induced Incandescence (TiRe-LII) for soot primary particle sizing in flames. Proceedings of the Combustion Institute, 2015, 35, 3673-3680.	3.9	45

Graham J Nathan

#	Article	IF	CITATIONS
37	The performance of a Solar Aided Power Generation plant with diverse "configuration-operation― combinations. Energy Conversion and Management, 2016, 124, 155-167.	9.2	45
38	Mixing Characteristics of a Flapping Jet from a Self-Exciting Nozzle. Flow, Turbulence and Combustion, 2001, 67, 1-23.	2.6	44
39	The effect of exit strain rate on soot volume fraction in turbulent non-premixed jet flames. Proceedings of the Combustion Institute, 2017, 36, 889-897.	3.9	42
40	Alternative carriers for remote renewable energy sources using existing CNG infrastructure. International Journal of Hydrogen Energy, 2010, 35, 1321-1329.	7.1	41
41	Simultaneous imaging of temperature and soot volume fraction. Proceedings of the Combustion Institute, 2011, 33, 791-798.	3.9	41
42	Effect of heliostat design wind speed on the levelised cost of electricity from concentrating solar thermal power tower plants. Solar Energy, 2015, 115, 441-451.	6.1	41
43	The relative performance of alternative oxygen carriers for liquid chemical looping combustion and gasification. International Journal of Hydrogen Energy, 2017, 42, 16396-16407.	7.1	40
44	The effect of oxygen concentration in the co-flow of laminar ethylene diffusion flames. Combustion and Flame, 2020, 211, 96-111.	5.2	40
45	Impact of the operation of non-displaced feedwater heaters on the performance of Solar Aided Power Generation plants. Energy Conversion and Management, 2017, 135, 1-8.	9.2	39
46	The effects of temperature and hydrodynamics on the crystallization fouling under cross flow conditions. Applied Thermal Engineering, 2012, 36, 210-218.	6.0	38
47	Preliminary evaluation of a novel solar bubble receiver for heating a gas. Solar Energy, 2019, 182, 264-277.	6.1	38
48	The energetic performance of a novel hybrid solar thermal & chemical looping combustion plant. Applied Energy, 2014, 132, 74-85.	10.1	36
49	Thermodynamic potential of molten copper oxide for high temperature solar energy storage and oxygen production. Applied Energy, 2017, 201, 69-83.	10.1	36
50	Performance Assessment of Fischer–Tropsch Liquid Fuels Production by Solar Hybridized Dual Fluidized Bed Gasification of Lignite. Energy & Fuels, 2015, 29, 2738-2751.	5.1	35
51	Solar-driven alumina calcination for CO ₂ mitigation and improved product quality. Green Chemistry, 2017, 19, 2992-3005.	9.0	34
52	Research challenges in combustion and gasification arising from emerging technologies employing directly irradiated concentrating solar thermal radiation. Proceedings of the Combustion Institute, 2017, 36, 2055-2074.	3.9	34
53	Effect of a uniform electric field on soot in laminar premixed ethylene/air flames. Combustion and Flame, 2010, 157, 1308-1315.	5.2	33
54	A hybrid solar chemical looping combustion system with a high solar share. Applied Energy, 2014, 126, 69-77.	10.1	33

#	Article	IF	CITATIONS
55	Phase-averaged velocity in a fluidic precessing jet nozzle and in its near external field. Experimental Thermal and Fluid Science, 2003, 27, 515-524.	2.7	32
56	Concentric multilayer model of the arc in high intensity discharge lamps for solar simulators with experimental validation. Solar Energy, 2015, 122, 293-306.	6.1	32
57	Measurement and prediction of NOx emissions from unconfined propane flames from turbulent-jet, bluff-body, swirl, and precessing jet burners. Proceedings of the Combustion Institute, 2000, 28, 481-487.	3.9	31
58	Planar laser-induced incandescence of turbulent sooting flames: the influence of beam steering and signal trapping. Applied Physics B: Lasers and Optics, 2015, 119, 731-743.	2.2	31
59	Experimental investigation of acoustic forcing on temperature, soot volume fraction and primary particle diameter in non-premixed laminar flames. Combustion and Flame, 2017, 181, 270-282.	5.2	31
60	High temperature solar thermochemical process for production of stored energy and oxygen based on CuO/Cu 2 O redox reactions. Solar Energy, 2017, 153, 1-10.	6.1	31
61	Concentrating or non-concentrating solar collectors for solar Aided Power Generation?. Energy Conversion and Management, 2017, 152, 281-290.	9.2	31
62	Corrections to facilitate planar imaging of particle concentration in particle-laden flows using Mie scattering, Part 1: Collimated laser sheets. Applied Optics, 2007, 46, 5823.	2.1	30
63	Mixed mode operation for the Solar Aided Power Generation. Applied Thermal Engineering, 2018, 139, 177-186.	6.0	30
64	The effect of exit Reynolds number on soot volume fraction in turbulent non-premixed jet flames. Combustion and Flame, 2018, 187, 42-51.	5.2	30
65	Effect of small vortex-generators on scalar mixing in the developing region of a turbulent jet. International Journal of Heat and Mass Transfer, 1999, 42, 3919-3926.	4.8	29
66	Hydrodynamic and chemical effects of hydrogen addition on soot evolution in turbulent nonpremixed bluff body ethylene flames. Proceedings of the Combustion Institute, 2017, 36, 807-814.	3.9	29
67	The Influence of Fuel Jet Precession on the Global Properties and Emissions of Unconfined Turbulent Flames. Combustion Science and Technology, 1996, 112, 211-230.	2.3	28
68	Storage capacities required for a solar thermal plant to avoid unscheduled reductions in output. Solar Energy, 2015, 118, 209-221.	6.1	28
69	An investigation into the effect of aspect ratio on the heat loss from a solar cavity receiver. Solar Energy, 2017, 149, 20-31.	6.1	28
70	The influence of geometric nozzle profile on the global properties of a turbulent diffusion flame. Proceedings of the Combustion Institute, 2007, 31, 1599-1607.	3.9	27
71	Potential of molten lead oxide for liquid chemical looping gasification (LCLG): A thermochemical analysis. International Journal of Hydrogen Energy, 2018, 43, 4195-4210.	7.1	27
72	Dynamic Modeling of the Coproduction of Liquid Fuels and Electricity from a Hybrid Solar Gasifier with Various Fuel Blends. Energy & Fuels, 2013, 27, 3556-3569.	5.1	26

#	Article	IF	CITATIONS
73	A Novel Solar Expanding-Vortex Particle Reactor: Experimental and Numerical Investigation of the Iso-thermal Flow Field and Particle Deposition. Solar Energy, 2016, 133, 451-464.	6.1	26
74	Similarity analysis of the momentum field of a subsonic, plane air jet with varying jet-exit and local Reynolds numbers. Physics of Fluids, 2013, 25, .	4.0	25
75	Effects of steam on the kinetics of calcium carbonate calcination. Chemical Engineering Science, 2021, 246, 116987.	3.8	25
76	Comparing the thermodynamic potential of alternative liquid metal oxides for the storage of solar thermal energy. Solar Energy, 2017, 157, 251-258.	6.1	25
77	The influence on the soot distribution within a laminar flame of radiation at fluxes of relevance to concentrated solar radiation. Combustion and Flame, 2011, 158, 1814-1821.	5.2	24
78	Thermodynamic potential of high temperature chemical looping combustion with molten iron oxide as the oxygen carrier. Chemical Engineering Research and Design, 2017, 120, 69-81.	5.6	24
79	Gasification Reactivity and Physicochemical Properties of the Chars from Raw and Torrefied Wood, Grape Marc, and Macroalgae. Energy & Fuels, 2017, 31, 2246-2259.	5.1	24
80	Impact of acoustic forcing on soot evolution and temperature in ethylene-air flames. Proceedings of the Combustion Institute, 2017, 36, 781-788.	3.9	24
81	Thermal performance of vortex-based solar particle receivers for sensible heating. Solar Energy, 2019, 177, 163-177.	6.1	24
82	The significance of particle clustering in pulverized coal flames. Proceedings of the Combustion Institute, 2002, 29, 797-804.	3.9	23
83	Self-excited jet-precession Strouhal number and its influence on downstream mixing field. Journal of Fluids and Structures, 2004, 19, 851-862.	3.4	23
84	Temperature measurements in turbulent non-premixed flames by two-line atomic fluorescence. Proceedings of the Combustion Institute, 2013, 34, 3619-3627.	3.9	23
85	Improvement of precision and accuracy of temperature imaging in sooting flames using two-line atomic fluorescence (TLAF). Combustion and Flame, 2016, 167, 481-493.	5.2	23
86	Experimental demonstration of the hybrid solar receiver combustor. Applied Energy, 2018, 224, 426-437.	10.1	23
87	Influence of nozzle diameter on soot evolution in acoustically forced laminar non-premixed flames. Combustion and Flame, 2018, 194, 376-386.	5.2	23
88	Large–Scale Dynamics of an Unconfined Precessing Jet Flame. Combustion Science and Technology, 1997, 126, 71-95.	2.3	22
89	Soot sheet dimensions in turbulent nonpremixed flames. Combustion and Flame, 2011, 158, 2458-2464.	5.2	22
90	The use of turbulence generators to mitigate crystallization fouling under cross flow conditions. Desalination, 2012, 288, 108-117.	8.2	22

6

#	Article	IF	CITATIONS
91	Corrections to facilitate planar imaging of particle concentration in particle-laden flows using Mie scattering Part 2: Diverging laser sheets. Applied Optics, 2007, 46, 7227.	2.1	21
92	Assessment of the potential benefits and constraints of a hybrid solar receiver and combustor operated in the MILD combustion regime. Energy, 2016, 116, 735-745.	8.8	21
93	Analytical assessment of a novel hybrid solar tubular receiver and combustor. Applied Energy, 2016, 162, 298-307.	10.1	21
94	Comparison of system performance in a hybrid solar receiver combustor operating with MILD and conventional combustion. Part II: Effect of the combustion mode. Solar Energy, 2017, 147, 479-488.	6.1	21
95	Ash–Bed Material Interaction during the Combustion and Steam Gasification of Australian Agricultural Residues. Energy & Fuels, 2018, 32, 4278-4290.	5.1	21
96	Experimental insights into the mechanism of heat losses from a cylindrical solar cavity receiver equipped with an air curtain. Solar Energy, 2020, 201, 314-322.	6.1	21
97	The effect of initial conditions on the exit flow from a fluidic precessing jet nozzle. Experiments in Fluids, 2004, 36, 70-81.	2.4	20
98	Instantaneous Temperature Imaging of Diffusion Flames Using Two-Line Atomic Fluorescence. Applied Spectroscopy, 2010, 64, 173-176.	2.2	20
99	Influence of the Type of Oxygen Carriers on the Performance of a Hybrid Solar Chemical Looping Combustion System. Energy & Fuels, 2014, 28, 2914-2924.	5.1	20
100	Global characteristics of non-premixed jet flames of hydrogen–hydrocarbon blended fuels. Combustion and Flame, 2015, 162, 1326-1335.	5.2	20
101	Comparison of system performance in a hybrid solar receiver combustor operating with MILD and conventional combustion. Part I: Solar-only and combustion-only employing conventional combustion. Solar Energy, 2017, 147, 489-503.	6.1	20
102	Experimental investigation of the effects of wind speed and yaw angle on heat losses from a heated cavity. Solar Energy, 2018, 165, 178-188.	6.1	20
103	Impact of start-up and shut-down losses on the economic benefit of an integrated hybrid solar cavity receiver and combustor. Applied Energy, 2016, 164, 10-20.	10.1	19
104	Experimental and numerical investigation of the flow characteristics within a Solar Expanding-Vortex Particle Receiver-Reactor. Solar Energy, 2017, 141, 25-37.	6.1	19
105	Thermal performance analysis of a syngas-fuelled hybrid solar receiver combustor operated in the MILD combustion regime. Combustion Science and Technology, 2019, 191, 2-17.	2.3	19
106	Reduced NOx emissions and enhanced large scale turbulence from a precessing jet burner. Proceedings of the Combustion Institute, 1992, 24, 1399-1405.	0.3	18
107	Solvent effects on two-line atomic fluorescence of indium. Applied Optics, 2010, 49, 1257.	2.1	18
108	Flow seeding with elemental metal species via an optical method. Applied Physics B: Lasers and Optics, 2012, 107, 665-668.	2.2	18

#	Article	IF	CITATIONS
109	The influence of high intensity solar radiation on the temperature and reduction of an oxygen carrier particle in hybrid chemical looping combustion. Chemical Engineering Science, 2013, 95, 331-342.	3.8	18
110	Temperature imaging of turbulent dilute spray flames using two-line atomic fluorescence. Experiments in Fluids, 2014, 55, 1.	2.4	18
111	Algorithm for soot sheet quantification in a piloted turbulent jet non-premixed natural gas flame. Experiments in Fluids, 2014, 55, 1.	2.4	18
112	System Optimization for Fischer–Tropsch Liquid Fuels Production via Solar Hybridized Dual Fluidized Bed Gasification of Solid Fuels. Energy & Fuels, 2017, 31, 2033-2043.	5.1	18
113	Experimental investigation of the reduction of liquid bismuth oxide with graphite. Fuel Processing Technology, 2019, 188, 110-117.	7.2	18
114	Assessment of interferences to nonlinear two-line atomic fluorescence (NTLAF) in sooty flames. Applied Physics B: Lasers and Optics, 2011, 104, 189-198.	2.2	17
115	PTV measurement of drag coefficient of fibrous particles with large aspect ratio. Powder Technology, 2012, 229, 261-269.	4.2	17
116	Mechanism for laser-induced fluorescence signal generation in a nanoparticle-seeded flow for planar flame thermometry. Applied Physics B: Lasers and Optics, 2015, 118, 209-218.	2.2	17
117	Thermogravimetric analysis of Cu, Mn, Co, and Pb oxides for thermochemical energy storage. Journal of Energy Storage, 2019, 23, 138-147.	8.1	17
118	The thermo-chemical potential liquid chemical looping gasification with bismuth oxide. International Journal of Hydrogen Energy, 2019, 44, 8038-8050.	7.1	17
119	Planar measurements of soot volume fraction and OH in a JP-8 pool fire. Combustion and Flame, 2009, 156, 1480-1492.	5.2	16
120	The influences of particle mass loading on mean and instantaneous particle distributions in precessing jet flows. International Journal of Multiphase Flow, 2012, 41, 13-22.	3.4	16
121	Approaches to accommodate resource variability in the modelling of solar driven gasification processes for liquid fuels synthesis. Solar Energy, 2017, 156, 101-112.	6.1	16
122	A method for identifying and characterising particle clusters in a two-phase turbulent jet. International Journal of Multiphase Flow, 2017, 88, 191-204.	3.4	16
123	An experimental study of the stability and performance characteristics of a Hybrid Solar Receiver Combustor operated in the MILD combustion regime. Proceedings of the Combustion Institute, 2019, 37, 5687-5695.	3.9	16
124	Precessing jet burners for stable and low NOx pulverised fuel flames — preliminary results from small-scale trials. Fuel, 1998, 77, 1013-1016.	6.4	15
125	The naturally oscillating flow emerging from a fluidic precessing jet nozzle. Journal of Fluid Mechanics, 2008, 606, 153-188.	3.4	15
126	New Seeding Methodology for Gas Concentration Measurements. Applied Spectroscopy, 2012, 66, 803-809.	2.2	15

8

#	Article	IF	CITATIONS
127	Soot evolution and flame response to acoustic forcing of laminar non-premixed jet flames at varying amplitudes. Combustion and Flame, 2018, 198, 249-259.	5.2	15
128	Resolving the three-dimensional structure of particles that are aerodynamically clustered by a turbulent flow. Physics of Fluids, 2019, 31, .	4.0	15
129	The influence of wall temperature distribution on the mixed convective losses from a heated cavity. Applied Thermal Engineering, 2019, 155, 157-165.	6.0	15
130	Effects of gas preheat temperature on soot formation in co-flow methane and ethylene diffusion flames. Proceedings of the Combustion Institute, 2021, 38, 1225-1232.	3.9	15
131	Puffing Frequency and Soot Extinction Correlation in JP-8 and Heptane Pool Fires. Combustion Science and Technology, 2008, 180, 699-712.	2.3	14
132	Numerical modelling of flows in a solar-enhanced vortex gasifier: Part 1, comparison of turbulence models. Progress in Computational Fluid Dynamics, 2015, 15, 114.	0.2	14
133	Effect of High-Flux Solar Irradiation on the Gasification of Coal in a Hybrid Entrained-Flow Reactor. Energy & Fuels, 2016, 30, 5138-5147.	5.1	14
134	Particle residence time distributions in a vortex-based solar particle receiver-reactor: An experimental, numerical and theoretical study. Chemical Engineering Science, 2020, 214, 115421.	3.8	14
135	The influence of inlet flow condition on the frequency of self-excited jet precession. Journal of Fluids and Structures, 2006, 22, 129-133.	3.4	13
136	A method to provide statistical measures of large-scale instantaneous particle clusters from planar images. Experiments in Fluids, 2011, 51, 641-656.	2.4	13
137	Techno-economic assessment of a hybrid solar receiver and combustor. AIP Conference Proceedings, 2016, , .	0.4	13
138	Combined solar energy and combustion of hydrogen-based fuels under MILD conditions. International Journal of Hydrogen Energy, 2018, 43, 20086-20100.	7.1	13
139	The influence of wind speed, aperture ratio and tilt angle on the heat losses from a finely controlled heated cavity for a solar receiver. Renewable Energy, 2019, 143, 1544-1553.	8.9	13
140	Solar Hybridized Coal-to-liquids via Gasification in Australia: Techno-economic Assessment. Energy Procedia, 2015, 69, 1819-1827.	1.8	12
141	Particle residence time distributions in a vortex-based solar particle receiver-reactor: The influence of receiver tilt angle. Solar Energy, 2019, 190, 126-138.	6.1	12
142	The energetic performance of a liquid chemical looping cycle with solar thermal energy storage. Energy, 2019, 170, 93-101.	8.8	12
143	Experimental assessment of copper oxide for liquid chemical looping for thermal energy storage. Journal of Energy Storage, 2019, 21, 216-221.	8.1	12
144	Simultaneously calibrated two-line atomic fluorescence for high-precision temperature imaging in sooting flames. Proceedings of the Combustion Institute, 2019, 37, 1417-1425.	3.9	12

#	Article	IF	CITATIONS
145	Experimental and numerical study of the influence of syngas composition on the performance and stability of a laboratory-scale MILD combustor. Experimental Thermal and Fluid Science, 2020, 115, 110083.	2.7	12
146	A mathematical model to assess the influence of transients on a refractory-lined solar receiver. Renewable Energy, 2021, 167, 217-235.	8.9	12
147	A MODIFIED THRING–NEWBY SCALING CRITERION FOR CONFINED, RAPIDLY SPREADING, AND UNSTEADY JETS. Combustion Science and Technology, 2005, 177, 1421-1447.	2.3	11
148	Assessment of the release of atomic Na from a burning black liquor droplet using quantitative PLIF. Combustion and Flame, 2009, 156, 1471-1479.	5.2	11
149	Simultaneous measurement of the surface temperature and the release of atomic sodium from a burning black liquor droplet. Combustion and Flame, 2010, 157, 769-777.	5.2	11
150	The potential role of data-centres in enabling investment in geothermal energy. Applied Energy, 2012, 98, 458-466.	10.1	11
151	Fischer-tropschliquid Fuel Production by Co-gasification of Coal and Biomass in a Solar Hybrid Dual Fluidized Bed Gasifier. Energy Procedia, 2015, 69, 1770-1779.	1.8	11
152	The influence of high flux broadband irradiation on soot concentration and temperature of a sooty flame. Combustion and Flame, 2016, 171, 103-111.	5.2	11
153	lso-thermal flow characteristics of rotationally symmetric jets generating a swirl within a cylindrical chamber. Physics of Fluids, 2018, 30, 055110.	4.0	11
154	Low kinetic-energy loss oscillating-triangular-jet nozzles. Experimental Thermal and Fluid Science, 2003, 27, 553-561.	2.7	10
155	The influences of jet precession on large-scale instantaneous turbulent particle clusters. International Journal of Multiphase Flow, 2011, 37, 394-402.	3.4	10
156	Storage capacity assessment of liquid fuels production by solar gasification in a packed bed reactor using a dynamic process model. Applied Energy, 2016, 173, 578-588.	10.1	10
157	Experimental and numerical investigation of the iso-thermal flow characteristics within a cylindrical chamber with multiple planar-symmetric impinging jets. Physics of Fluids, 2017, 29, 105111.	4.0	10
158	The flow-field within a vortex-based solar cavity receiver with an open aperture. Experimental Thermal and Fluid Science, 2021, 123, 110314.	2.7	10
159	The influence of aspect ratio on distributions of settling velocities and orientations of long fibres. Powder Technology, 2014, 257, 192-197.	4.2	9
160	Velocity and orientation distributions of fibrous particles in the near-field of a turbulent jet. Powder Technology, 2015, 276, 10-17.	4.2	9
161	Techno-economic evaluation of modular hybrid concentrating solar power systems. Energy, 2017, 129, 158-170.	8.8	9
162	Effect of Calcium and Phosphorus on Interactions between Quartz Sand and K-Salt-Doped Wood under Both Steam Gasification and Combustion Atmospheres. Energy & Fuels, 2020, 34, 3210-3222.	5.1	9

#	Article	IF	CITATIONS
163	Flow regimes within horizontal particle-laden pipe flows. International Journal of Multiphase Flow, 2021, 143, 103748.	3.4	9
164	The role of fuel-rich clusters in flame stabilization and NOx emission reduction with precessing jet pulverized fuel flames. Proceedings of the Combustion Institute, 1998, 27, 3173-3179.	0.3	8
165	The effect of density ratio on the near field of a naturally occurring oscillating jet. Experiments in Fluids, 2010, 48, 69-80.	2.4	8
166	Analytical assessment of a novel rotating fluidized bed solar reactor for steam gasification of char particles. Solar Energy, 2016, 140, 113-123.	6.1	8
167	Impact of Flow Blowing and Suction strategies on the establishment of an aerodynamic barrier for solar cavity receivers. Applied Thermal Engineering, 2020, 180, 115841.	6.0	8
168	Interactions between Quartz Sand and Wood Doped with either K or Na Salts under Steam Gasification and Combustion Atmospheres. Industrial & Engineering Chemistry Research, 2020, 59, 1712-1722.	3.7	8
169	Particle velocity measurement within a free-falling particle curtain using microscopic shadow velocimetry. Optics Express, 2021, 29, 10923.	3.4	8
170	Numerical and experimental analysis of poly-dispersion effects on particle-laden jets. International Journal of Heat and Fluid Flow, 2021, 91, 108852.	2.4	8
171	The influence of the coefficient of restitution on flow regimes within horizontal particle-laden pipe flows. Physics of Fluids, 2021, 33, .	4.0	8
172	Investigation of a combustion driven oscillation in a refinery flare. Part A: Full scale assessment. Experimental Thermal and Fluid Science, 2006, 30, 285-295.	2.7	7
173	The influences of jet precession on near field particle distributions. International Journal of Multiphase Flow, 2009, 35, 288-296.	3.4	7
174	RANS modeling of a particulate turbulent round jet. Chemical Engineering Science, 2010, 65, 3384-3393.	3.8	7
175	Influence of droplet size on the release of atomic sodium from a burning black liquor droplet in a flat flame. Fuel, 2010, 89, 1840-1848.	6.4	7
176	Aerodynamics of long fibres settling in air at 10 <re<100. 2013,="" 235,="" 550-555.<="" powder="" td="" technology,=""><td>4.2</td><td>7</td></re<100.>	4.2	7
177	Non-intrusive temperature measurement of particles in a fluidised bed heated by well-characterised radiation. International Journal of Multiphase Flow, 2018, 100, 186-195.	3.4	7
178	Luminescence interference to two-colour toluene laser-induced fluorescence thermometry in a particle-laden flow. Experiments in Fluids, 2020, 61, 1.	2.4	7
179	Influence of particle loading, Froude and Stokes number on the global thermal performance of a vortex-based solar particle receiver. Renewable Energy, 2022, 184, 201-214.	8.9	7
180	The Effect of Reynolds Number on the Passive Scalar Field in the Turbulent Wake of a Circular Cylinder. Flow, Turbulence and Combustion, 2004, 72, 311-331.	2.6	6

#	Article	IF	CITATIONS
181	Development of ASTRI high-temperature solar receivers. AIP Conference Proceedings, 2017, , .	0.4	6
182	The influence of aspect ratio on the iso-thermal flow characteristics of multiple confined jets. Physics of Fluids, 2018, 30, 125108.	4.0	6
183	A new correlation between soot sheet width and soot volume fraction in turbulent non-premixed jet flames. Proceedings of the Combustion Institute, 2019, 37, 927-934.	3.9	6
184	Soot-flowfield interactions in turbulent non-premixed bluff-body flames of ethylene/nitrogen. Proceedings of the Combustion Institute, 2021, 38, 1125-1132.	3.9	6
185	THE ROLE OF PROCESS AND FLAME INTERACTION IN REDUCING NOx EMISSIONS. , 1995, , 309-318.		6
186	Bottom-Up Estimates of the Cost of Supplying High-Temperature Industrial Process Heat from Intermittent Renewable Electricity and Thermal Energy Storage in Australia. Processes, 2022, 10, 1070.	2.8	6
187	Scaling of the gas phase in particle-laden turbulent axisymmetric jets. International Journal of Multiphase Flow, 2009, 35, 96-100.	3.4	5
188	Influence of a combustion-driven oscillation on global mixing in the flame from a refinery flare. Experimental Thermal and Fluid Science, 2011, 35, 199-210.	2.7	5
189	Single-shot planar temperature imaging of radiatively heated fluidized particles. Optics Express, 2017, 25, 28764.	3.4	5
190	Assessing the techno-economics of modular hybrid solar thermal systems. AIP Conference Proceedings, 2017, , .	0.4	5
191	Characteristics of swirling and precessing flows generated by multiple confined jets. Physics of Fluids, 2019, 31, 055102.	4.0	5
192	Temperature imaging of mobile BaMgAl10017:Eu phosphor aggregates under high radiation flux. Optics and Lasers in Engineering, 2021, 137, 106398.	3.8	5
193	Generating planar distributions of soot particles from luminosity images in turbulent flames using deep learning. Applied Physics B: Lasers and Optics, 2021, 127, 1.	2.2	5
194	Insights from a new method providing single-shot, planar measurement of gas-phase temperature in particle-laden flows under high-flux radiation. Experiments in Fluids, 2021, 62, 1.	2.4	5
195	Integration assessment of the hybrid sulphur cycle with a copper production plant. Energy Conversion and Management, 2021, 249, 114832.	9.2	5
196	First-of-a-kind investigation on performance of a directly-irradiated windowless vortex-based particle receiver. AIP Conference Proceedings, 2020, , .	0.4	5
197	Investigation of a combustion driven oscillation in a refinery flare. Experimental Thermal and Fluid Science, 2007, 31, 1091-1101.	2.7	4
198	Particleâ€5cale Investigation of Heat Transfer in Radiationâ€Driven Char Gasification. Chemical Engineering and Technology, 2016, 39, 1903-1911.	1.5	4

#	Article	IF	CITATIONS
199	Secondary Concentrators to Achieve High Flux Radiation With Metal Halide Solar Simulators. Journal of Solar Energy Engineering, Transactions of the ASME, 2016, 138, .	1.8	4
200	Calculated concentration distributions and time histories of key species in an acoustically forced laminar flame. Combustion and Flame, 2019, 204, 189-203.	5.2	4
201	Numerical investigation of the isothermal flow field and particle deposition behaviour in a rotating fluidized bed solar receiver. Solar Energy, 2019, 182, 348-360.	6.1	4
202	Technical feasibility of integrating concentrating solar thermal energy in the Bayer alumina process. AIP Conference Proceedings, 2020, , .	0.4	4
203	In-situ imaging of particle size distribution in an industrial-scale calcination reactor using micro-focusing particle shadowgraphy. Powder Technology, 2022, 404, 117459.	4.2	4
204	Non-gaussian statistics of a passive scalar in turbulent flows. Proceedings of the Combustion Institute, 1998, 27, 989-995.	0.3	3
205	Development of the ASTRI heliostat. AIP Conference Proceedings, 2016, , .	0.4	3
206	The Topology of a Precessing Flow Within a Suddenly Expanding Axisymmetric Chamber. Journal of Fluids Engineering, Transactions of the ASME, 2017, 139, .	1.5	3
207	Gas-lift circulation of a liquid between two inter-connected bubble columns. Chemical Engineering Science, 2020, 218, 115574.	3.8	3
208	Experimental investigation of the influence of solar-to-fuel ratio on performance and stability characteristics of hybrid solar-MILD hydrogen processes. Proceedings of the Combustion Institute, 2021, 38, 6723-6731.	3.9	3
209	Statistical relationship between soot volume fraction, temperature, primary particle diameter and OH radicals along transects normal to the local reaction zone in a turbulent flame. Proceedings of the Combustion Institute, 2021, 38, 1497-1505.	3.9	3
210	Experimental investigation on the influence of an air curtain on the convective heat losses from solar cavity receivers under windy condition. AIP Conference Proceedings, 2020, , .	0.4	3
211	Measured global thermal performance of a directly irradiated suspension-flow solar particle receiver with an open aperture. Solar Energy, 2022, 231, 185-193.	6.1	3
212	Influence of sidewalls on the centerline small-scale turbulence of a turbulent high-aspect-ratio rectangular jet. Experimental Thermal and Fluid Science, 2014, 58, 139-144.	2.7	2
213	New Understanding of Mode Switching in the Fluidic Precessing Jet Flow. Journal of Fluids Engineering, Transactions of the ASME, 2017, 139, .	1.5	2
214	The coupling between the internal and external flows through a hybridized solar cavity receiver under isothermal conditions. Experimental Thermal and Fluid Science, 2020, 113, 110028.	2.7	2
215	Renormalisation of particle distributions in an initially-biased turbulent jet by swirl and radial injection. International Journal of Multiphase Flow, 2021, 135, 103509.	3.4	2
216	Direct measurements and prediction of the particle egress from a vortex-based solar cavity receiver with an open aperture. Solar Energy, 2022, 235, 105-117.	6.1	2

#	Article	IF	CITATIONS
217	Influence of stoichiometry on the release of atomic sodium from a burning black liquor droplet in a flat flame with and without boron. Fuel, 2010, 89, 2608-2616.	6.4	1
218	A Modified Thermodynamic Model to Estimate the Performance of Geothermal Aided Power Generation Plant. Advanced Materials Research, 0, 347-353, 2875-2878.	0.3	1
219	Optical thermometry for high temperature multiphase environments under high-flux irradiation. Solar Energy, 2017, 146, 191-198.	6.1	1
220	Flow behavior inside a novel rotating fluidized bed for solar gasification of biomass. AIP Conference Proceedings, 2017, , .	0.4	1
221	Performance of a hybrid solar receiver combustor. AIP Conference Proceedings, 2018, , .	0.4	1
222	Performance characteristics of a hybrid solar receiver combustor utilising hydrogen or syngas. AIP Conference Proceedings, 2019, , .	0.4	1
223	Hybrid Solar-MILD Combustion for Renewable Energy Generation. Frontiers in Mechanical Engineering, 2019, 5, .	1.8	1
224	A technical assessment of pneumatic conveying of solids for a high temperature particle receiver. AIP Conference Proceedings, 2019, , .	0.4	1
225	An adaptive aerodynamic approach to mitigate convective losses from solar cavity receivers. Solar Energy, 2021, 224, 1333-1343.	6.1	1
226	The effect of particle size and volumetric loading on the gas temperature distributions in a particle-laden flow heated with high-flux radiation. International Journal of Heat and Mass Transfer, 2022, 182, 122041.	4.8	1
227	Editorial: Technological and Fundamental Advances in Production, Storage and Utilization of Fuels. Frontiers in Energy Research, 2022, 10, .	2.3	1
228	On the use of oscillating jet flames in a coflow to develop soot models for practical applications. Proceedings of the Combustion Institute, 2021, 38, 1309-1317.	3.9	0
229	Optics and Photonics in Solar Thermal Energy Technologies. , 2014, , .		0
230	The Dynamic Performance of Different Configurations of Solar Aided Power Generation (SAPG). , 2016, , .		0
231	First-of-a-kind demonstration of a direct hybrid between a solar receiver and the radiant burner technology. AIP Conference Proceedings, 2020, , .	0.4	Ο
232	The effect of instantaneous particle distributions on the gas-phase temperature in an unsteady particle-laden jet heated with high-flux radiation. International Journal of Multiphase Flow, 2022, 153, 104106.	3.4	0